To appear in *Proceedings of XXI Moriond Conference: Galaxy Clusters and the High Redshift Universe Observed in X-rays*, edited by D. Neumann, F. Durret, & J. Tran Thanh Van, in press

MERGER SHOCKS AND NONTHERMAL PROCESSES IN CLUSTERS OF GALAXIES

CRAIG L. SARAZIN
Department of Astronomy, University of Virginia, P. O. Box 3818, Charlottesville, VA 22903-0818, U.S.A.

Clusters of galaxies generally form by the gravitational merger of smaller clusters and groups. Major cluster mergers are the most energetic events in the Universe since the Big Bang. Mergers drive shocks into the intracluster gas, and these shocks heat the intracluster gas, and should also accelerate nonthermal relativistic particles. The thermal effects of merger shocks will be briefly discussed. Mergers can increase the temperature and X-ray luminosities of clusters, and this may affect statistical conclusions about cosmological parameters. As a result of particle acceleration in shocks, clusters of galaxies should contain very large populations of relativistic electrons and ions. Electrons with Lorentz factors $\gamma \sim 300$ (energies $E = \gamma m_e c^2 \sim 150$ MeV) are expected to be particularly common. Observations and models for the radio, extreme ultraviolet, hard X-ray, and gamma-ray emission from nonthermal particles accelerated in these shocks will also be described. The predicted gamma-ray fluxes of clusters should make them easily observable with GLAST. Chandra X-ray observations of the interaction between the radio lobes and cooling flow gas in Abell 2052 are also discussed briefly.

1 Introduction

Major cluster mergers are the most energetic events in the Universe since the Big Bang. Cluster mergers are the mechanism by which clusters are assembled. In these mergers, the subclusters collide at velocities of ∼2000 km/s, releasing gravitational binding energies of as much as $\gtrsim 10^{64}$ ergs. Figure 1 shows the Chandra image of the merging cluster Abell 85, which has two subclusters merging with the main cluster.[46] Spectral measurements show that the southern subcluster is merging at a relative velocity of about 2800 km/s.

The relative motions in mergers are moderately supersonic, and shocks are driven into the intracluster medium. In major mergers, these hydrodynamical shocks dissipate energies of $\sim 3 \times 10^{63}$ ergs; such shocks are the major heating source for the X-ray emitting intracluster medium. The shock velocities in merger shocks are similar to those in supernova remnants in our Galaxy, and we expect them to produce similar effects. Mergers shocks should heat and compress the X-ray emitting intracluster gas, and increase its entropy. We also expect that particle acceleration by these shocks will produce nonthermal electrons and ions, and these can produce synchrotron radio, inverse Compton (IC) EUV and hard X-ray, and gamma-ray emission.

Hydrodynamical simulations of cluster formation and evolution have shown the importance of merger shocks.[80,72] The evolution of the structure of merger shocks is illustrated in Figure 2,[70] which shows an off-center merger between two symmetric subclusters. At early stages in the merger (the first panel and earlier), the shocked region is located between the two subcluster

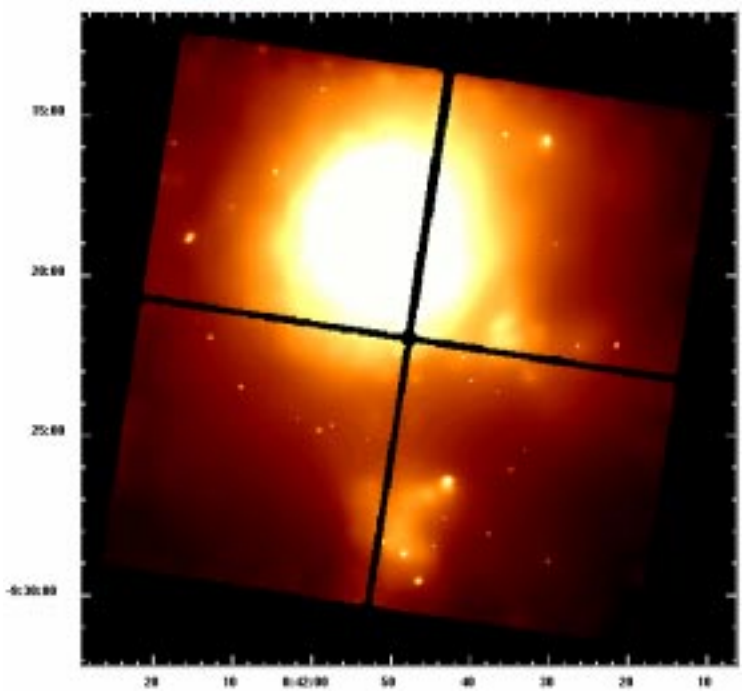

Figure 1: The Chandra ACIS-I image of the merger cluster Abell 85.[46] The false color scale burns out the central cooling flow region to show the outer parts of the cluster. Two subclusters to the south and southwest are merging with the main cluster. The southwestern subcluster has a radio relic, and the southern subcluster also has a diffuse radio source which may be a relic.[2] The sharp feature at the northwest of the southern subcluster is a "cold front".[87]

centers and is bounded on either side by two shocks. At this time, the subcluster centers, which may contain cooling cores and central radio sources, are not affected. Later, these shocks sweep over the subcluster centers (between the first and second panels); the survival of central cool cores depends on how sharply peaked the potentials of the subclusters are.[54,70] The main merger shocks pass into the outer parts of the merging system (panel 2), and secondary shocks may appear in the inner regions (panel 3). Eventually, the cluster begins to return to equilibrium (panel 4).

2 Thermal Effects of Merger Shocks

Merger shocks heat and compress the intracluster gas, and these effects can be used to determine the geometry and kinematics of the merger.[54] Recently, Chandra images have detected a number of merger shock regions in clusters.[53,55] Merger shocks can also mix the intracluster medium.

2.1 Mergers and Cooling Flows

Merger shocks also appear to disrupt cooling flows. There is a strong statistical anticorrelation between cooling flows and/or cooling rates, and irregular structures in clusters as derived by statistical analysis of their X-ray images.[17] It is unlikely that this is due to shock heating of the cooling flow gas.[29,40,70,76] Numerical simulations and physical arguments suggest that the disruption may be due to the ram pressure of the gas from the other subcluster.[29,40,54,70,76] The cooling flow gas is displaced from the potential minimum, and eventually mixes with hotter, more diffuse gas. Figure 3 shows the results of a numerical simulation of an offset merger between subclusters with a mass ratio of about 1:3.[70] The color scale shows the specific entropy of the gas in the center of one of the subclusters. Initially, the ram pressure of the merging

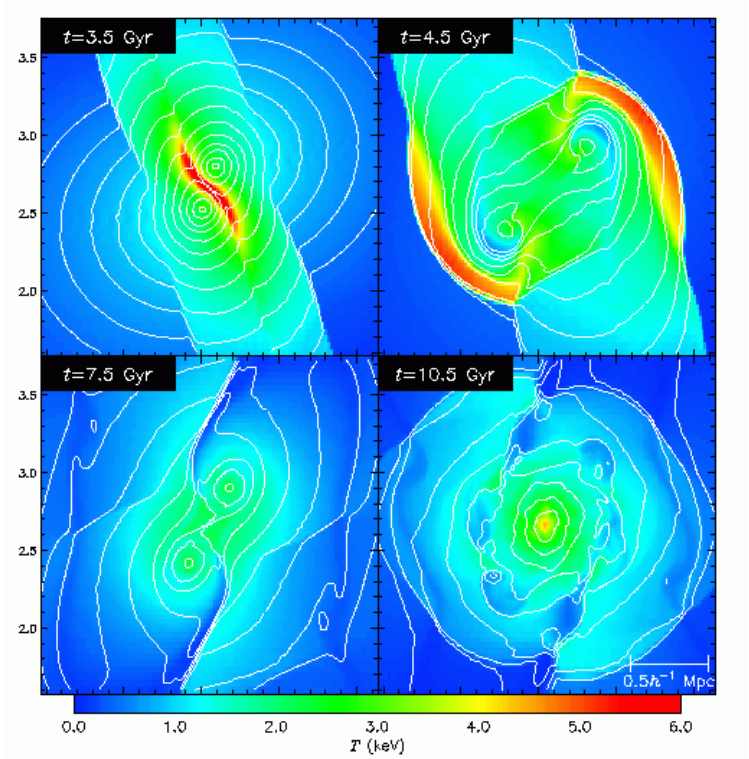

Figure 2: The results of a hydro simulation of a symmetric, off-center merger by Ricker and Sarazin.[70] The colors show the temperature, while the contours are the X-ray surface brightness. Initially, the shocked region is located between the two subcluster centers. Later, the main merger shocks propogate to the outer parts of the cluster, and other weaker shocks also occur. By the end of the simulation, the cluster is beginning to return to equilibrium.

subcluster gas displaces the lower entropy gas from the center of the potential, causing it to become convectively unstable. The resulting convective plumes produce large-scale turbulent motions with eddy sizes up to several 100 kpc. This mixing eventually eliminates the lower entropy gas at the cluster core.

Assuming that ram pressure is the main mechanism for disrupting cooling flows in mergers, one expects that the merger will remove the cooling flow gas at radii which satisfy

$$\rho_{\rm sc} v_{\rm rel}^2 \gtrsim P_{\rm CF}(r)\,, \tag{1}$$

where $P_{\rm CF}(r)$ is the pressure profile in the cooling flow, $\rho_{\rm sc}$ is the density of the merging subcluster gas at the location of the cooling flow, and $v_{\rm rel}$ is the relative velocity of the merging subcluster gas and the cooling flow. Gòmez et al. (2001) find that this relation provides a reasonable approximation to the disruption in their simulations. The pressure profile in the cooling flow gas prior to the merger is determined by the condition of hydrostatic equilibrium. If the cluster gravitational potential has a wide core within which the potential is nearly constant (e.g., as in a King model), then the cooling flow pressure will not increase rapidly into the center. In this case, once the merger reaches the central regions of the cluster, if the ram pressure is sufficient to remove the outer parts of the cooling flow, it should be sufficient to remove nearly all of the cooling flow. On the other hand, if the cluster potential is sharply peaked (as in a NFW profile[61]), the merger may remove the outer parts of the cooling flow but not the innermost regions. Thus, the survival and size of cool cores in merging clusters can provide evidence on whether clusters have sharply peaked potentials.[54]

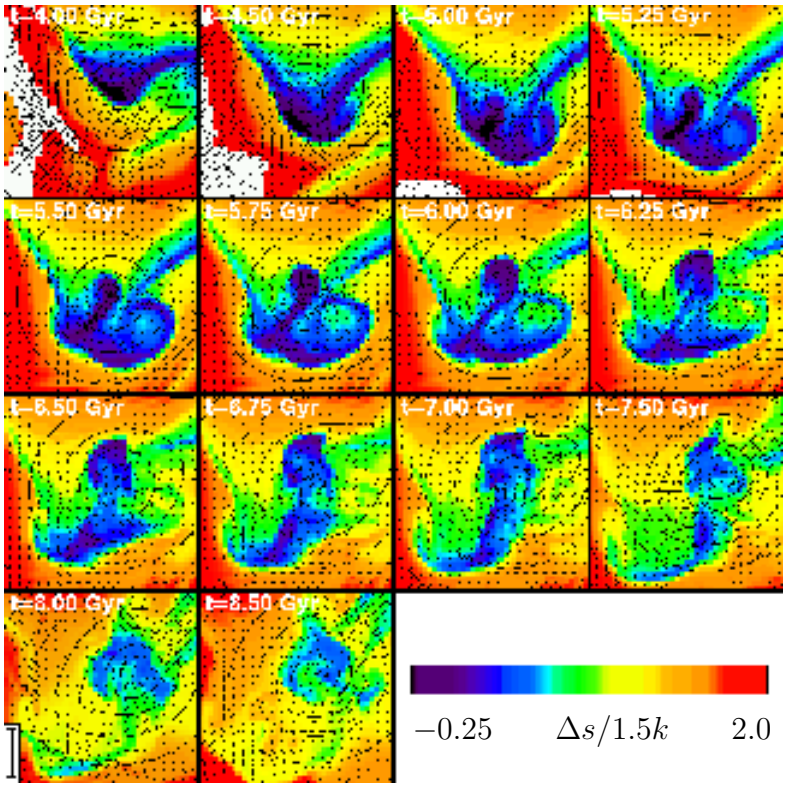

Figure 3: A merger-driven convective plume mixing the low entropy gas at the core of a cluster with higher entropy surrounding gas.[70] The plots show the specific entropy (entropy per particle) in units of $(3/2)k$ in the inner $\sim$600 h^{-1} kpc square of a merging cluster simulation at a series of time steps covering about 4.5 Gyr. Blue colors are low entropy gas, while red and white colors are high entropy.

2.2 Luminosity and Temperature Boosts in Mergers

The compression and heating associated with merger shocks boosts the X-ray luminosity and temperature of the intracluster gas. Figure 4 shows the variation in the 2–10 keV X-ray luminosity L_X and the average emission-weighted X-ray temperature T_X as functions of the time t in simulations of the merger of equal mass subclusters.[70] The three curves are for different values for the impact parameter for the collision; the solid curve is for a head-on collision. The values of L_X and T_X are normalized to the sum of the two subclusters prior to the merger. The merger can increase the X-ray luminosity of the sum of the two subclusters by a factor of $\sim$10 ($\sim$20 times the initial individual luminosities of the subclusters). The X-ray temperature can be increased by a factor of $\sim$3.

The most massive, luminous, and hottest clusters are relatively rare. For relaxed, virialized clusters, the Press-Schechter formalism predicts that the abundance of clusters drops exponentially with mass for the largest systems.[47,66] The X-ray luminosity and temperature boosts during rare major merger events are large enough to strongly affect the statistics of the hottest and most X-ray luminous clusters. Thus, one might expect that the most X-ray luminous and hottest clusters would mainly be mergers.[67] There are a number of examples which support this argument. The cluster 1E 0657-56 = RXJ0658-5557 is probably the hottest known cluster, with a temperature of $kT \approx 16$ keV.[85,53] The Chandra image of this cluster reveals a complex merger with a spectacular bow shock.[53] Similarly, Abell 2163 may be the second hottest known cluster; its Chandra image shows two apparent shock regions.[56] Abell 665, one of the most X-ray luminous clusters at redshift $z \lesssim 0.2$, is currently undergoing a merger, and may be near the time of core collision[39] when the L_X and T_X boosts are the largest.[70] The Chandra image shows

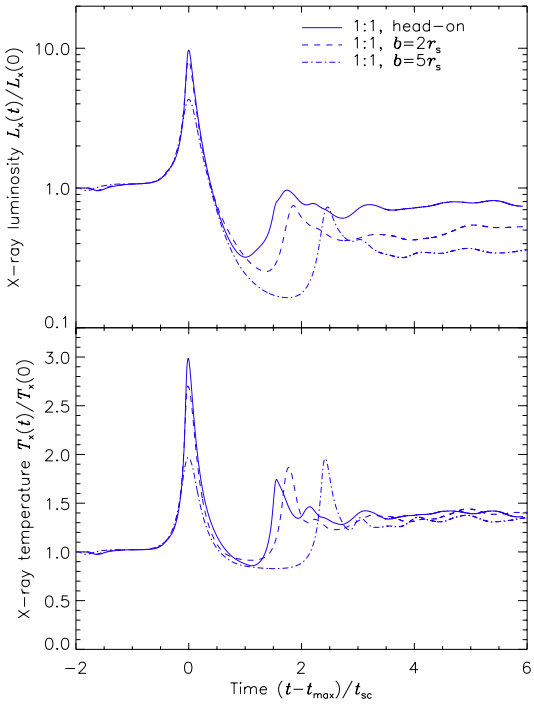

Figure 4: The X-ray luminosity L_X (2–10 keV) and average emission-weighted X-ray temperature T_X as functions of time t in merger simulations for equal mass subclusters.[70] The luminosity and temperature are for the total system (both subclusters) and are scaled to their initial values. Time is offset from the time of peak luminosity $t_{\rm max}$ and scaled to the sound-crossing time $t_{\rm sc}$ for each subcluster. The three curves are for different values of the impact parameter b for the collision.

a dramatic merger shock.[53,56] The very distant, luminous, and hot cluster MS1054-03 shows evidence of substructure indicative of an ongoing merger.[62]

There is a strong, steep correlation between the radio luminosity of clusters with radio halos, and their X-ray temperature and/or luminosity.[48,32] This relationship is steeper than might be expected from simple scaling arguments in clusters.[45] Since radio halos are only observed in clusters undergoing mergers[31,81], and may be powered by merger shock acceleration (§ 3.4), the strong correlation with the X-ray temperature and luminosity may be due, in part, to the merger boost in these quantities. This might explain why radio observations of Sunyaev-Zel'dovich clusters, which are generally selected to be brightest and hottest clusters, have found the (otherwise relatively rare) radio halos in a number of cases.[60,48]

The abundance of massive clusters at moderately large redshifts has been used as an important diagnostic for the matter density in the Universe and Ω_M.[63,86,3,22] Since it is difficult to determine the mass directly, the X-ray temperature or luminosity is often used in its place, and the observations are usually analyzed assuming that the clusters are relaxed and virialized. In Press-Schechter theory, the abundance of massive clusters declines rapidly with mass and with redshift, and the rate of decline with redshift increase rapidly with Ω_M. Thus, the presence of hot, X-ray luminous clusters at significant redshifts (e.g., MS1054-03) provides an upper limit on Ω_M which excludes the Einstein-de Sitter Universe.[3,22] However, if most of these clusters are undergoing mergers, their masses may be overestimated and their abundance underestimated by these equilibrium arguments. Thus, mergers may bias the inferred value of Ω_M to lower values.[67]

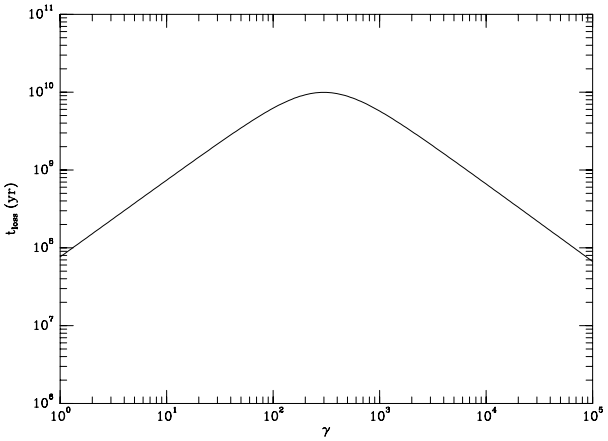

Figure 5: The loss time scale for relativistic electrons in a cluster of galaxies under typical intracluster conditions as a function of their Lorentz factor γ. The particles have energies of $E = \gamma m_e c^2$.

3 Particle Acceleration and Nonthermal Emission

3.1 Shock Acceleration

Radio observations of supernova remnants indicate that shocks with $v \gtrsim 10^3$ km/s convert at least a few percent of the shock energy into the acceleration of relativistic electrons.[15] Even more energy may go into relativistic ions. While the merger shocks in cluster have lower Mach numbers and compressions than the blast waves in young supernova remnants, it is probable that shock acceleration operates efficiently in clusters as well. Given that all of the thermal energy of the intracluster gas in clusters is due to shocks with such velocities, it seems likely that relativistic electrons with a total energy of $\gtrsim 10^{62}$ ergs are produced in clusters, with perhaps even higher energies in ions.

Clusters are also very good storage locations for cosmic rays. Under reasonable assumptions for the diffusion coefficient, particles with energies $\lesssim 10^6$ GeV have diffusion times which are longer than the Hubble time.[5,20] Figure 5 gives the loss time scales for relativistic electrons under typical intracluster conditions. Although high energy electrons lose energy rapidly due to IC and synchrotron emission, electrons with Lorentz factors of $\gamma \sim 300$ (energies ~ 150 MeV) have long lifetimes which approach the Hubble time.[74,78] Thus, clusters of galaxies can retain low energy electrons ($\gamma \sim 300$) and nearly all cosmic ray ions for a significant fraction of a Hubble time.

I have calculated models for the relativistic electrons in clusters, assuming they are primary electrons accelerated in merger shocks.[74,75] An alternative theory is that these particles are secondaries produced by the decay of charged mesons generated in cosmic ray ion collisions.[20] Two recent cluster merger simulations have included particle acceleration approximately.[71,84] Their conclusions are very similar to mine based on simpler models. The populations of cosmic ray electrons in clusters depends on their merger histories. Because low energy electrons have long lifetimes, one expects to find a large population of them in most clusters (any cluster which has had a significant merger since $z \sim 1$). On the other hand, higher energy electrons ($E \gtrsim 1$ GeV) have short lifetimes (shorter than the time for a merger shock to cross a cluster). Thus, one only expects to find large numbers of higher energy electrons in clusters which are having or have just had a merger.

Fig. 6(a) shows the electron spectrum in a cluster with a typical history. Most of the electron energy is in electrons with $\gamma \sim 300$, which have the longest lifetimes. These electrons are produced by mergers over the entire history of the cluster. This cluster also has a small ongoing merger which produces the high energy tail on the electron distribution.

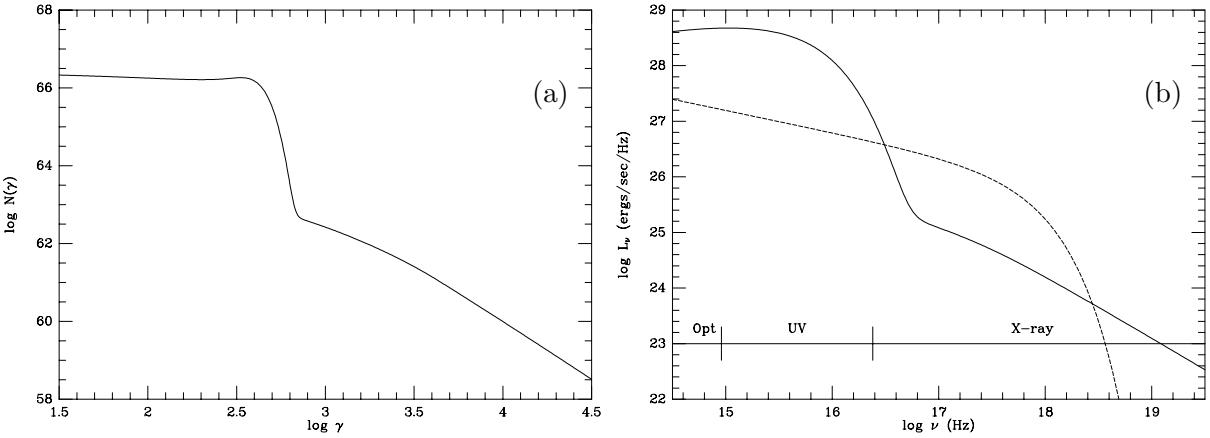

Figure 6: (a) A typical model for the relativistic electron population in a cluster of galaxies. The lower energy electrons are due to all of the mergers in the cluster history, while the high energy electrons are due to a small current merger. (b) The IC spectrum from the same model (solid curve). The dashed curve is a 7 keV thermal bremsstrahlung spectrum.

Energetically, most of the emission from these electrons is due to IC, and the resulting spectrum is shown in Fig. 6(b). For comparison, thermal bremsstrahlung with a typical rich cluster temperature and luminosity is shown as a dashed curve. Fig. 6(b) shows that clusters should be strong sources of extreme ultraviolet (EUV) radiation. Since this emission is due to electrons with $\gamma \sim 300$ which have very long lifetimes, EUV radiation should be a common feature of clusters.[78]

In clusters with an ongoing merger, the higher energy electrons will produce a hard X-ray tail via IC scattering of the Cosmic Microwave Background (CMB); the same electrons will produce diffuse radio synchrotron emission.

3.2 EUV/Soft X-ray Emission

Excess EUV emission has apparently been detected with the EUVE satellite in six clusters (Virgo, Coma, Abell 1795, Abell 2199, Abell 4038, & Abell 4059).[49,50,13,59,14,42,51,52,6,12,7] In fact, the EUVE satellite appears to have detected all of the clusters it observed which are nearby, which have long integration times, and which lie in directions of low Galactic column where detection is possible at these energies. However, the EUV detections and claimed properties of the clusters remain quite controversial.[13,1,14,6]

The EUV observations suggest that rich clusters generally have EUV luminosities of $\sim 10^{44}$ ergs/s, and have spectra which decline rapidly in going from the EUV to the X-ray band. The EUV emission is very spatially extended.

While it is possible that the EUV emission may be thermal in origin,[28,12] I believe that it is more likely that this emission is due to inverse Compton scattering (IC) of CMB photons by low energy relativistic electrons.[41,13,25,78] In this model, the EUV would be produced by electrons with energies of $\sim$150 MeV ($\gamma \sim 300$; Fig. 6). As noted above, these electrons have lifetimes which are comparable to the Hubble time, and should be present in essentially all clusters. This can explain why EUV emission is common. To produce the EUV luminosities observed, one needs a population of such electrons with a total energy of $\sim 10^{62}$ ergs, which is about 3% of the typical thermal energy content of clusters. This is a reasonable acceleration efficiency for these particles, given that both the thermal energy in the intracluster gas and the relativistic particles result from merger shocks. The steep spectrum in going from EUV to X-ray bands is predicted by this model [Fig. 6(b)], it results from the rapid increase in losses ($\propto \gamma^2$) for particles as the energy increases above $\gamma \sim 300$ (Fig. 5).

The broad spatial distribution of the EUV is also naturally explained by the density depen-

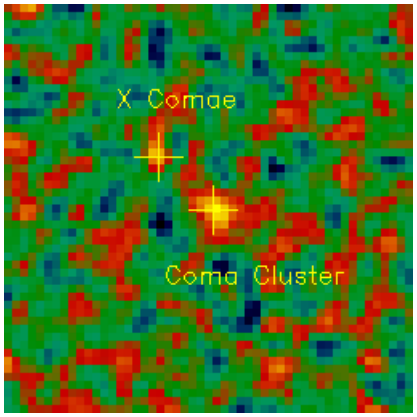

Figure 7: A simulated INTEGRAL–IBIS image of the hard X-ray emission from the Coma cluster in the 40–120 keV band.[38] Such observations can separate the cluster emission from that of the nearby AGN X-Comae, and can determine a crude radial distribution for the emission.

dence of IC emission. The thermal emission which produces the bulk of the X-ray emission in clusters is due to collisions between thermal electrons and ions; thus, it declines with the square of the density as the radius increases. On the other hand, IC emission is due to collisions between cosmic ray electrons and CMB photons; since the CMB energy density is extremely uniform, IC EUV emission varies with a single power of density, rather than density squared. This simple difference can explain why the EUV is more extended than the thermal X-ray emission.

3.3 Hard X-ray Tails

If clusters contain higher energy relativistic electrons with $\gamma \sim 10^4$, these particles will produce hard X-ray (HXR) emission by IC scattering, and radio synchrotron emission depending on the intracluster magnetic field. Since these higher energy electrons have short lifetimes, they should only be present in clusters with evidence for a recent or ongoing merger.

Because of the short lifetimes of the electrons producing HXR IC emission, the population of these particles should be close to steady-state. The emitting electrons would have a nearly power-law energy distribution with an exponent which is one power steeper than that of the accelerated particles.[36] The HXR luminosity should be proportional to the energy input from particle acceleration due to the cluster merger. To a good approximation, the present day value of $L_{\rm HXR}$ (20–100 keV) is simply given by[74]

$$L_{\rm HXR} \approx 0.17 \dot{E}_{\rm CR,e}(\gamma > 5000)\,. \qquad (2)$$

where $\dot{E}_{\rm CR,e}(\gamma > 5000)$ is the total present rate of injection of energy in cosmic ray electrons with $\gamma > 5000$. If the relativistic electrons are accelerated in merger shocks, then $\dot{E}_{\rm CR,e}(\gamma > 5000)$ should just be proportional to the rate of energy dissipation in shocks.

Hard X-ray emission in excess of the thermal emission and detected as a nonthermal tail at energies $\gtrsim$20 keV has been seen in at least two clusters. The Coma cluster, which is undergoing at least one merger and which has a radio halo, was detected with both BeppoSAX and RXTE.[34,69] BeppoSAX also has detected Abell 2256;[35] another merger cluster with strong diffuse radio emission. BeppoSAX may have detected Abell 2199,[42] although I believe the evidence is less compelling for this case. A nonthermal IC hard X-ray detection of Abell 2199 would be surprising, as this cluster is very relaxed and has no radio halo or relic.[44]

The ratio of hard X-ray IC emission to radio synchrotron emission allows one to determine the magnetic field in clusters.[68,34,35] The present HXR detections lead to average mag-

netic fields which are rather low ($\sim$0.2 μG)[34,35]) compared to the values from Faraday rotation measurements[33,19]

An alternative explanation of the hard X-ray tails is that they might be due to nonthermal bremsstrahlung,[27,10,21,77] which is bremsstrahlung from nonthermal electrons with energies of 10–1000 keV which are being accelerated to higher energies. However, it may be difficult to produce a sufficient nonthermal tail on the electron distribution.[65]

The previous hard X-ray detections of clusters have been done with instruments with very poor angular resolution. Thus, they provide no information on the distribution of the hard X-ray emission. It would be very useful to determine if the hard X-ray emission is localized to the radio emitting regions in clusters. For clusters with radio relics, these might be associated with the positions of merger shocks in the X-ray images. Better angular resolution would also insure that the hard X-ray detections of clusters are not contaminated by emission from other sources. The IBIS instrument on INTEGRAL will provide a hard X-ray capability with better angular resolution, and may allow the hard X-ray emission regions to be imaged.[38] Figure 7 shows a simulation of an IBIS observation of the Coma cluster.

The predicted IC emission from nonthermal particles is much weaker than the thermal emission in the central portion of the X-ray band from about 0.3 keV to 20 keV [Fig. 6(b)], However, if the IC emission is localized to merger shock regions, its local surface brightness might be comparable to the thermal X-ray emission. A possible detection of localized IC emission associated with merger shocks and radio relics has been claimed in Abell 85.[2] It is possible that Chandra and XMM/Newton will find IC emission associated with other merger shocks and radio relics.

3.4 Radio Halos and Relics

A number of clusters of galaxies are known to contain large-scale diffuse radio sources which have no obvious connection to individual galaxies in the cluster.[37] They also have very steeply declining radio spectra. These sources are referred to as radio halos when they appear projected on the center of the cluster, and are called relics when they are found on the cluster periphery (although they have other distinctive properties). The best known and studied radio halo is in the Coma cluster.[23] These radio halos and relics are relatively uncommon; about 40 are known at the present time. Although radio halos and relics have been studied for some time, lately the number of known cases has increased dramatically. This is largely due to the radio surveys (like NVSS and WENSS) and new low frequency radio instruments. Perhaps the largest number of new sources have come from the NVSS survey and VLA pointed observation follow up effort by Giovannini, Feretti, and collaborators.[37] Other new detections have involved other VLA surveys,[64] the VLA at 74 MHz,[43] SUMSS and MOST,[73] the ATCA,[48] and WENSS.[45]

In all cases of which I am aware, they have been found in clusters which show significant evidence for an ungoing merger.[37,31,32,81,16] This suggests that the relativistic electrons are accelerated by merger shocks. In the early stages of mergers, halos are often found on the border between the subclusters, where the cluster gas is first being shocked (e.g., Abell 85).[82] In more advanced mergers, more conventional centrally located halos (e.g., Coma) and peripheral relics (e.g., Abell 3667) are found. Abell 3667 provides a spectacular case of two bow-shaped radio relics at opposite sides of a merging cluster,[73] and located at the positions where merger shocks are predicted.[71] Recent Chandra X-ray images of two clusters with radio halos and mergers (Abell 665 and Abell 2163) show evidence for a simple connection between the shocked regions and the radio emission.[56]

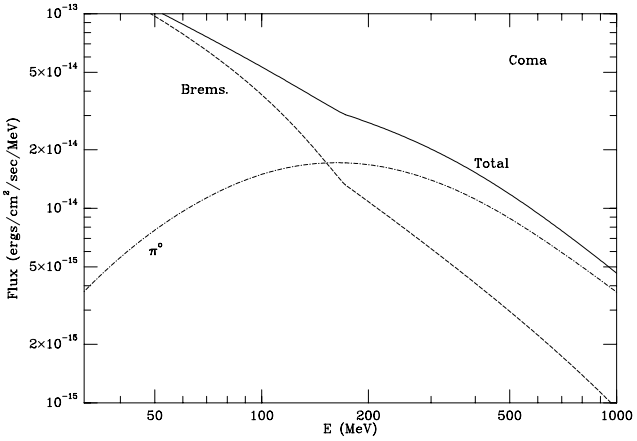

Figure 8: The predicted gamma-ray spectrum for the Coma cluster, including electron bremsstrahlung and π^o decay from ions.[75]

3.5 Predicted Gamma-Ray Emission

Relativistic electrons and ions in clusters are also expected to produce strong gamma-ray emission.[26,20,11,9,75,24] The region near 100 MeV is particularly interesting, as this region includes bremsstrahlung from the most common electrons with $\gamma \sim 300$, and gamma-rays from ions produced by π^o decay. Both of these processes involve collisions between relativistic particles (electrons for bremsstrahlung, ions for π^o emission) and thermal particles, so they should both vary in the same way with density in the cluster. Thus, the ratio of these two spectrally distinguishable emission processes should tell us the ratio of cosmic ray ions to electrons in clusters.[9,75]

Figure 8 shows the predicted gamma-ray spectrum for the Coma cluster, based on a model which reproduces the observed EUV, hard X-ray, and radio emission.[75] The observed upper limit from CGO/EGRET is $<4 \times 10^{-8}$ cts/cm^2/s for $E > 100$ MeV;[83] while the predicted value for this model is $\sim 2 \times 10^{-8}$ cts/cm^2/s. The EGRET upper limit already shows that the ratio of ions to electrons cannot be too large ($\lesssim 30$).[9,75] The predicted fluxes are such that many nearby clusters should be easily detectable with GLAST.

4 Radio Source / Cooling Flow Interaction in Abell 2052

Although it is not really covered by my assigned topic, I cannot resist the opportunity to show some new results from our Chandra observation of the cooling flow cluster Abell 2052.[8] (Since this involves the interaction of the "nonthermal" radio source with the X-ray gas, perhaps it just fits under my title.) Abell 2052 is a moderately rich, cooling flow cluster at a redshift of $z = 0.0348$. The central cD in this cluster hosts the powerful, complex radio source 3C 317. Abell 2052 was observed with *Chandra* on 2000 September 3 for a total of 36,754 seconds. The smoothed X-ray image and radio contours are shown in Figure 9. There is an X-ray point source coincident with the radio AGN. The AGN lies just above an East-West bar of X-ray emission. The extended radio emission corresponds with "holes" in the X-ray emission, and the radio source is surrounded by a brightened "shell" of X-ray emission. In the northern X-ray hole / radio lobe, there is a "spur" of X-ray emission sticking into the hole. The X-ray shell around the southern radio lobe is incomplete at the bottom. The X-ray hole / radio lobe structure is very similar to that seen with Chandra in Hydra A;[57] Perseus;[30] Abell 2597;[58] and possibly RBS797.[79]

The pressure in the X-ray-bright gas is nearly continuous with the pressure of the surrounding gas. There is no clear evidence for strong shocks. Thus, it seems likely that the radio lobes are displacing and compressing the X-ray gas, but are, at the same time, confined by the X-ray gas.

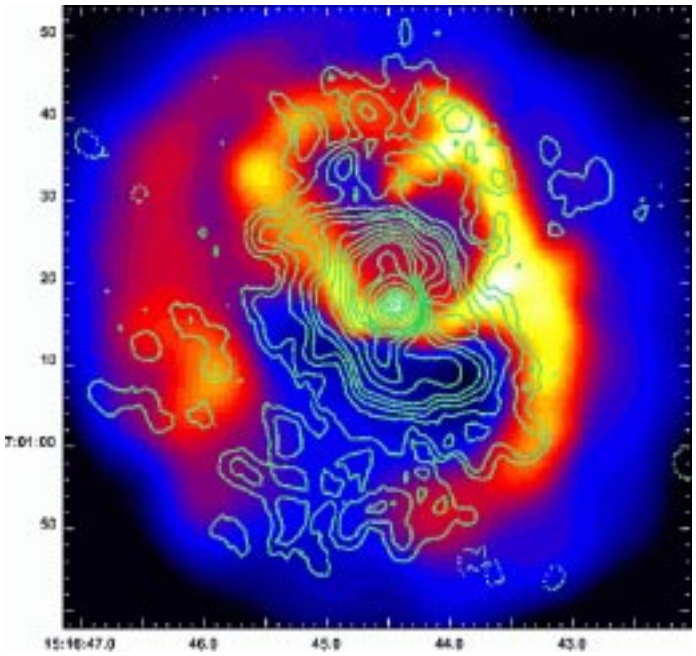

Figure 9: The color image shows the central $\sim 80'' \times 80''$ region of an adaptively smoothed version of the 0.3–10 keV Chandra image of the center of Abell 2052.[8] The green contours are the 6 cm radio image.[18]

The minimum nonthermal pressure in the radio lobes is about an order of magnitude smaller than that in the X-ray shell and surrounding thermal gas. Thus, it is likely that the usual equipartition arguments fail for this (and presumably other) radio sources. The radio lobes might be supported by pressure from low energy relativistic electrons, relativistic ions, magnetic fields, or very hot, low density thermal gas.

Contours of Hα + [N II] emission[4] are plotted over the smoothed X-ray emission in Figure 10. Optical emission lines are seen from the AGN, from the East-West bar, and from the brightest portions of the shell, including the spur. The compression of the X-ray shell by the radio source appear to have promoted cooling, including to low temperatures $\sim 10^4$ K. A deeper optical line image might reveal emission from the remainder of the X-ray shell.

Acknowledgments

I want to thank my collaborators Liz Blanton, Josh Kempner, Maxim Markevitch, Scott Randall, Paul Ricker, and Alexey Vikhlinin for all their help. Liz Blanton, Paolo Goldoni, Josh Kempner, and Paul Ricker kindly provided figures for this paper. Support for this work was provided by the National Aeronautics and Space Administration through Chandra Award Numbers GO0-1119X, GO0-1173X, GO0-1158X, and GO1-2122X, issued by the Chandra X-ray Observatory Center, which is operated by the Smithsonian Astrophysical Observatory for and on behalf of NASA under contract NAS8-39073. Support also came from NASA XMM grants NAG 5-10074 and NAG 5-10075.

References

1. Arabadjis, J. S., & Bregman, J. N. 1999, ApJ, 514, 607
2. Bagchi, J., Pislar, V., & Lima Neto, G. B. 1998, MNRAS, 296, L23
3. Bahcall, N. A., & Fan, X. 1998, ApJ, 504, 1

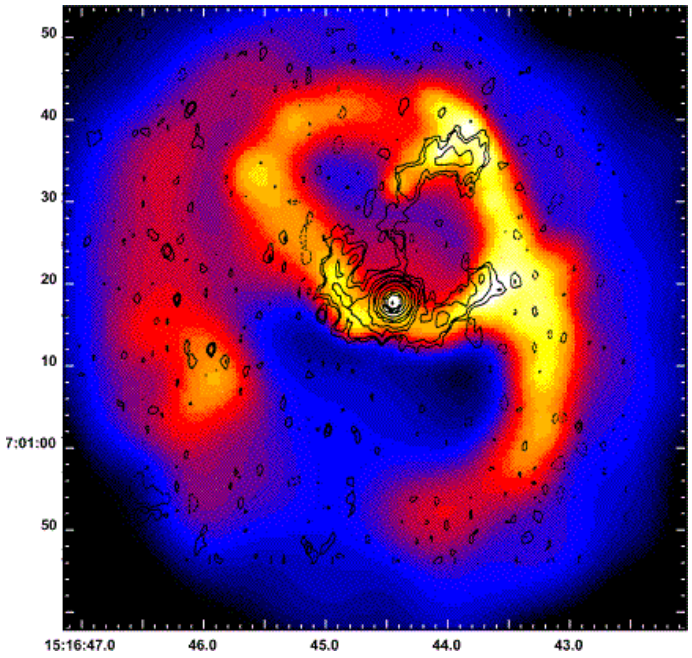

Figure 10: Overlay of the Hα + [N II] contours[4] onto the central $\sim 80'' \times 80''$ X-ray image of Abell 2052.[8]

4. Baum, S. A., Heckman, T. M., Bridle, A., van Breugel, W. J. M., & Miley, G. K. 1988, ApJS, 68, 643
5. Berezinsky, V. S., Blasi, P., & Ptuskin, V. S. 1997, ApJ, 487, 529
6. Berghöfer, T. W., Bowyer, S., & Korpela, E. 2000, ApJ, 535, 615
7. Berghöfer, T. W., Bowyer, S., & Korpela, E. 2000b, ApJ, 545, 695
8. Blanton, E. L., Sarazin, C. L., McNamara, B. R., & Wise, M. W. 2001, ApJL, submitted
9. Blasi, P. 1999, ApJ, 525, 603
10. Blasi, P. 2000, ApJ, 532, L9
11. Blasi, P., & Colafrancesco, S. 1999, APh, 12, 169
12. Bonamente, M., Lieu, R., & Mittaz, J. 2001, ApJ, 547, L7
13. Bowyer, S., & Berghöfer, T. W. 1998, ApJ, 506, 502
14. Bowyer, S., Berghöfer, T. W., & Korpela, E. 1999, ApJ, 526, 592
15. Blandford, R. D., & Eichler, D. 1987, Phys. Rep., 154, 1
16. Buote, D. A. 2001, ApJL, in press (astro-ph/0104211)
17. Buote, D. A., & Tsai, J. C. 1996, ApJ, 458, 27
18. Burns, J. O. 1990, AJ, 99, 14
19. Clarke, T. E., Kronberg, P. P., & Böhringer, H. 2001, ApJ, 547, L111
20. Colafrancesco, S., & Blasi, P. 1998, APh, 9, 227
21. Dogiel, V. A. 2000, A&A, 357, 66
22. Donahue, M., & Voit, G. M. 1999, ApJ, 523, L137
23. Deiss, B. M., Reich, W., Lesch, H., & Wielebinski, R. 1997, A&A, 321, 55
24. Dolag, K., & Enßlin, T. A. 2000, A&A, 362, 151
25. Enßlin, T. A., & Biermann, P. L. 1998, A&A, 330, 90
26. Enßlin, T. A., Biermann, P. L., Kronberg, P. P., & Wu, X.-P. 1997, ApJ, 477, 560
27. Enßlin, T. A., Lieu, R. & Biermann, P. L. 1999 A&A, 344, 409
28. Fabian, A. C. 1997, Science, 275, 48
29. Fabian, A. C., & Daines, S. J. 1991, MNRAS, 252, 17p
30. Fabian, A. C., et al., 2000, MNRAS, 318, 65
31. Feretti, L. 1999, in Proc. Diffuse Thermal and Relativistic Plasma in Galaxy Clusters, ed.

H. Böhringer, L. Feretti, & P. Schuecker (Garching: MPE), 1
32. Feretti, L. 2001, in The Universe at Low Radio Frequencies, in press (astro-ph/0006379)
33. Feretti, L., Dallacasa, D., Giovannini, G., & Tagliani, A. 1995, A&A, 302, 6
34. Fusco-Femiano, R., et al., 1999, ApJ, 513, L21
35. Fusco-Femiano, R., et al., 2000, ApJ, 534, L7
36. Ginzburg, V. L., & Syrovatskii, S. I. 1964, The Origin of Cosmic Rays
37. Giovannini, G., et al., 1993, ApJ, 406, 399
38. Goldoni, P., Goldwurm, A., Laurent, P., Casse, M., Paul, J., & Sarazin, C. 2001. in INTEGRAL Science Workshop, in press (astro-ph/0102363)
39. Gómez, P. L., Hughes, J. P., & Birkinshaw, M. 2000, ApJ, 540, 726
40. Gómez, P. L., Loken, C., Roettiger, K., & Burns, J. O. 2001, ApJ, in press
41. Hwang, C.-Y. 1997, Science, 278, 1917
42. Kaastra, J. S., et al., 1999, ApJ, 519, L119
43. Kassim, N. E., Perley, R. A., & Erickson, W. C. 1999, in Proc. Diffuse Thermal and Relativistic Plasma in Galaxy Clusters, ed. H. Böhringer, L. Feretti, & P. Schuecker (Garching: MPE), 49
44. Kempner, J., & Sarazin, C. L. 2000, ApJ, 530, 282
45. Kempner, J., & Sarazin, C. L. 2001, ApJ, 548, 639
46. Kempner, J., Sarazin, C. L., & Ricker, P. R. 2001, preprint
47. Lacey, C., & Cole, S. 1993, MNRAS, 262, 627
48. Liang, H., Hunstead, R. W., Birkinshaw, M., & Andreani, P. 2000, ApJ, 544, 686
49. Lieu, R., et al., 1996, Science, 274, 1335
50. Lieu, R., et al., 1996, ApJ, 458, L5
51. Lieu, R., Bonamente, M., & Mittaz, J. 1999, ApJ, 517, L91
52. Lieu, R., et al., 1999, ApJ, 527, L77
53. Markevitch, M. 2001, in Proceeding of XXI Moriond Conference: Galaxy Clusters and the High Redshift Universe Observed in X-rays, ed. D. Neumann, F. Durret, & J. Tran Thanh Van, in press
54. Markevitch, M., Sarazin, C. L., & Vikhlinin, A. 1999, ApJ, 521, 526
55. Markevitch, M., Vikhlinin, A., Mazzotta, P., & Van Speybroeck, L. 2001, in X-ray Astronomy 2000, ed. R. Giacconi, L. Stella, & S. Serio (San Francisco: ASP), in press (astro-ph/0012215)
56. Markevitch, M., & Vikhlinin, A. 2001, ApJ, submitted
57. McNamara, B. R., et al., 2000, ApJ, 534, L135
58. McNamara, B. R., Wise, M. W., David, L. P., Nulsen, P. E. J, & Sarazin, C. L. 2001, in Constructing the Universe with Clusters of Galaxies, ed. F. Durret & D. Gerbal, astro-ph/0012331, http://www.iap.fr/Conferences/Colloque/coll2000/contributions/ /textes.pdf/mcnamara.pdf
59. Mittaz, J. P. D., Lieu, R., & Lockman, F. J. 1998, ApJ, 498, L17
60. Moffet, A. T., & Birkinshaw, M. 1989, AJ, 98, 1148
61. Navarro, J. F., Frenk, C. S., & White, S. D. M. 1997, ApJ, 490, 493
62. Neumann, D., & Arnaud, M. 2000, ApJ, 542, 35
63. Oukbir, J., & Blanchard, A. 1992, A&A, 262, L21
64. Owen, F. N., Morrison, G., & Voges, W. in Proc. Diffuse Thermal and Relativistic Plasma in Galaxy Clusters, ed. H. Böhringer, L. Feretti, & P. Schuecker (Garching: MPE), 9
65. Petrosian, V. 2001, ApJ, in press (astro-ph/0101145)
66. Press, W. H., & Schechter, P. 1974, ApJ, 187, 425
67. Randall, S. W., Sarazin, C. L., & Ricker, P. M. 2001, preprint
68. Rephaeli, Y. 1979, ApJ, 227, 364
69. Rephaeli, Y., Gruber, D., & Blanco, P. 1999, ApJ, 511, L21

70. Ricker, P. M., & Sarazin, C. L. 2001, ApJ, submitted
71. Roettiger, K., Burns, J., & Stone, J. M. 1999, ApJ, 518, 603
72. Roettiger, K., Stone, J. M., & Burns, J. 1999, ApJ, 518, 594
73. Röttgering, H., Wieringa, M., Hunstead, R., & Ekers, R. 1997, MNRAS, 290, 57
74. Sarazin, C. L. 1999a, ApJ, 520, 529
75. Sarazin, C. L. 1999b, in Proc. Diffuse Thermal and Relativistic Plasma in Galaxy Clusters, ed. H. Böhringer, L. Feretti, & P. Schuecker (Garching: MPE), 185
76. Sarazin, C. L. 2001, in Merging Processes in Clusters of Galaxies, ed. L. Feretti, I. M. Gioia, & G. Giovannini (Dordrecht: Kluwer), in press (astro-ph/0105418)
77. Sarazin, C. L., & Kempner, J. 2000, ApJ, 533, 73
78. Sarazin, C. L., & Lieu, R. 1998, ApJ, 494, L177
79. Schindler, S., Castillo-Morales, A., De Filippis, E., Schwope, A., & Wambsganss, J. 2001, A&A, preprint
80. Schindler, S., & Müller E. 1993, A&A, 272, 137
81. Schuecker, P., & Böhringer, H. 1999, in Proc. Diffuse Thermal and Relativistic Plasma in Galaxy Clusters, ed. H. Böhringer, L. Feretti, & P. Schuecker (MPE Rep. 271) (Garching: Max Planck Institut für Extraterrestrische Physik), 43
82. Slee, O. B., & Reynolds, J. E. 1984, PASA, 5, 516
83. Sreekumar, P., et al., 1996, ApJ, 464, 628
84. Takizawa, M., & Naito, T. 2000, ApJ, 535, 586
85. Tucker, W., et al., 1998, ApJ, 496, L5
86. Viana, P. T. P., & Liddle, A. R. 1996, MNRAS, 281, 323
87. Vikhlinin, A., Markevitch, M., & Murray, S. M. 2001, ApJ, 551, 160